PNAS RESEARCH ARTICLE | ENVIRONMENTAL SCIENCES

Coupling of excitation energy to photochemistry in natural marine phytoplankton communities under iron stress

Heshani Pupulewatte[a,b], Maxim Y. Gorbunov[b], C. Mark Moore[c], Corday R. Selden[b], Thomas J. Ryan-Keogh[d], Joe Furby[c], Ruth Hawley[c], Maeve C. Lohan[c], Thomas S. Bibby[c], and Paul G. Falkowski[a,b,1]

Affiliations are included on p. 7.

Contributed by Paul G. Falkowski; received May 13, 2025; accepted June 30, 2025; reviewed by Roberto Bassi and Robert L. Burnap

Oxygenic photosynthesis requires excitation energy transfer from light-harvesting complexes (LHCs) to reaction centers (RCs) to drive photochemical redox chemistry. The effective absorption cross section of RCs dynamically responds to the light environment on time scales of seconds to days, allowing rapid acclimations to changes in spectral irradiance and photoprotection under high light, thereby optimizing light absorption for photochemistry. Although energy coupling between LHC–RCs has been studied for decades in laboratory cultures, it remains poorly understood in real-world conditions, where it is potentially influenced by nutrients. In the oceans, one of the most critical micronutrients for photosynthesis is iron (Fe). To investigate the effects of Fe stress on the energetic coupling between LHC–RCs in natural phytoplankton assemblages in the Southern Atlantic Ocean, we assessed photophysiological responses using a pair of custom-built fluorometers measuring chlorophyll-a variable fluorescence and picosecond fluorescence lifetimes. Detailed analysis based on the functional absorption cross section of the oxygen-evolving complex, quantum yield of photochemistry, energetic connectivity of RCs, and the average lifetime of in vivo chlorophyll fluorescence suggested that between 10 and 25% of LHCs remain uncoupled from RCs and do not effectively contribute to photochemical charge separation. Addition of Fe to samples under trace metal-clean on-board incubations indicates relatively rapid recoupling (< 24 h) of antennae to photochemistry, followed by biophysical stabilization of recoupled complexes. Our findings highlight the crucial role of micronutrients in controlling the excitation energy transfer from LHCs to RCs in marine phytoplankton and the overall primary productivity in the real-world oceans.

photosynthesis | variable chlorophyll fluorescence | energy transfer | fluorescence lifetime | iron limitation

Significance

We examined the efficiency with which absorbed solar energy is transferred to photosynthetic electron flow in natural marine phytoplankton assemblages in the Southern Atlantic Ocean. Using a unique combination of variable fluorescence and fluorescence lifetime measurements, we measured the energetic interaction between light-harvesting complexes and reaction centers responsible for generating electrons in splitting water, and hence phytoplankton growth. Our results reveal that iron plays a critical role in restoring energy transfer through multifaceted mechanisms, including the recoupling of existing photosynthetic complexes and also the reassembly and repair of the photosynthetic apparatus. These findings underscore the importance of iron in the energetic coupling of solar energy to photochemistry and how phytoplankton adapt to changes in nutrient supply prevailing in real-world oceans.

All oxygenic photoautotrophs convert light into chemical bond energy through a suite of light-dependent reactions. The initial light-dependent reaction photochemically splits water with a specific, unique catalyst, Photosystem II (PSII). This process generates electrons and protons, which are ultimately used to reduce carbon dioxide, and depending on the environment, nitrate and sulfate (1). The first challenge photosynthetic organisms face is capturing light, which is a relatively dilute energy source, even in the upper ocean. Reaction centers (RCs), protein complexes responsible for charge separation, contain relatively few light-harvesting pigments; hence, they can absorb only a few photons each second. Indeed, without an increase in the functional absorption cross section of PSII (σ_{PSII}), oxygenic photosynthesis would be extremely slow (1–3). To increase photon capture, the RCs are energetically coupled to light-harvesting complexes (LHCs). These pigment-binding antenna complexes, which are themselves incapable of photochemistry, greatly increase the cross section of the RC, but only if they are energetically coupled (2).

Biophysically, LHCs act as energy funnels, in which typically shorter wavelengths of light are absorbed by peripheral LHCs. Excitation energy is transferred between pigments within the LHCs to RCs via Förster's resonant energy-transfer (FRET) mechanism. In 1946, Förster described the rate of energy transfer ($k_{Förster}$) between a donor and acceptor chromophore as dependent on the donor lifetime (τ_D), the quantum yield of the donor fluorescence (φ_D), the interchromophore distance (R), the relative orientation of the donor–acceptor pair (κ), and the overlap integral (J_F) (4). Recent studies focus on the development of new excitonic energy levels shared between strongly interacting molecules, which explain the quantum mechanical nature of excitation energy transfer (5). FRET occurs along a downhill energy gradient toward the RC, where charge separation is restricted by kinetics (3). Charge separation and stabilization should occur at a much faster rate than the decay of an excited-state chlorophyll *a* molecule (k_d). In nutrient-replete

Author contributions: M.Y.G., C.M.M., T.S.B., and P.G.F. designed research; H.P., C.M.M., C.R.S., T.J.R.-K., J.F., and R.H. performed research; M.Y.G., C.M.M., and M.C.L. contributed new reagents/analytic tools; H.P., M.Y.G., C.M.M., T.S.B., and P.G.F. analyzed data; and H.P., M.Y.G., C.M.M., C.R.S., T.J.R.-K., J.F., R.H., M.C.L., T.S.B., and P.G.F. wrote the paper.

Reviewers: R.B., Stazione Zoologica Anton Dohrn, Naples, Italy; and R.L.B., Oklahoma State University.

The authors declare no competing interest.

[1]To whom correspondence may be addressed. Email: falko@marine.rutgers.edu.

This article contains supporting information online at https://www.pnas.org/lookup/suppl/doi:10.1073/pnas.2511916122/-/DCSupplemental.

Published July 29, 2025.

oxygenic organisms, k_d averages ca. 0.5 ns^{-1} (6). However, if FRET impedes, the excess absorbed energy is dissipated either as heat or fluorescence (7, 8). Hence, the interactions between pigments within the LHCs, and the energetic coupling to the RCs, critically determine how efficiently absorbed solar energy is converted to electron flow.

Fine-tuning the energy transfer process between LHCs and RCs is essential for photosynthetic organisms to adapt to environmental variability, including light and nutrients (9–11). In the ocean, the paucity of nutrients, in particular, can lead to a substantial decrease in the photosynthetic electron transfer efficiency (12). Nearly every macromolecular complex in the electron transport chain in thylakoid membranes depends on Fe. Hence, Fe limitation significantly affects light harvesting and excitation transfer to RCs across 30 to 60% of the upper global ocean (13). The presence of uncoupled LHCs under Fe stress was initially studied by Riethman et al. (14) and Greene et al. (15). "Uncoupled" LHCs are defined as light-harvesting complexes that are unable to transfer excitation energy to the RCs. Although many of these studies were conducted in cyanobacteria (16), uncoupling has been observed in Fe-stressed laboratory cultures of the red alga, *Rhodella violacea* (17), the green algae, *Dunaliella tertiolecta* (18) and *Chlamydomonas reinhardtii* (19), and the diatom *Phaeodactylum tricornutum* (15). Lin et al. (20) were the first to document extraordinarily long in situ chlorophyll fluorescence lifetimes due to Fe stress in the global ocean, which they attributed to inactive RCs and uncoupled LHCs. However, little is known about how intermolecular energy transfer is affected by environmental conditions in natural phytoplankton communities.

Here, we report the effects of Fe stress on PSII functionality and FRET dynamics in natural and nutrient-amended marine phytoplankton communities of the South Atlantic Ocean collected on the Royal Research Ship (RRS) *Discovery* (expedition DY172) from December 21, 2023, to January 24, 2024. A total of 22 nutrient addition experiments were performed along a transect that extended south from the South African coast to the marginal ice zone of the Weddell Gyre then back to the South Atlantic subtropical gyre (Fig. 1*B*).

To assess FRET efficiency, we used two different custom-built fluorometers. The first measures the kinetics of variable chlorophyll fluorescence from microseconds to several milliseconds. This Fluorescence Induction Relaxation (FIRe) instrument is used to quantify the quantum yield photochemistry ($ø_P$), and a suite of associated characteristics including variable fluorescence, e.g., maximal fluorescence, F_m, minimal fluorescence, F_o, quantum yield of PSII photochemistry, F_v/F_m, functional absorption cross section of PSII, σ_{PSII}, and the connectivity of energy between RCs, ρ (23). The second is a picosecond lifetime fluorescence (PicoLiF) instrument, which measures the exponential decay of chlorophyll fluorescence (as quantified using the lifetime τ), in the picosecond to nanosecond time domain. This measurement allows for the quantification of the quantum yield of fluorescence ($ø_F$) in vivo. Both instruments are extremely sensitive; the measurements are obtained simultaneously and do not require filtration of natural phytoplankton assemblages. The latter is critical; in the open ocean, the average chlorophyll concentration in situ is ~0.2 μg/L and often less (24). Filtration takes many minutes to hours, during which time the relevant photosynthetic parameters can change significantly. Combining the two, independent fluorescence measurements allow closure on the energy budget of absorbed solar radiation in phytoplankton in situ based on the equations of Strasser and Butler's formalism (7, 12). The research presented here reveals that a significant population of LHCs are often poorly coupled energetically to photochemistry in situ due to Fe limitation.

Results

The Combination of Variable Chlorophyll Fluorescence and Picosecond Lifetimes Shows Signatures of Uncoupling of LHCs and RCs Under Severe Fe Stress. We examined photophysiology across the upper ocean from the high-latitude South Atlantic (60°S) to the eastern South Atlantic Gyre (Fig. 1). Nutrient addition experiments were conducted using various factorial combinations of inorganic Fe, Nitrogen (N), Phosphorus (P), and Manganese (Mn). Subsamples for photophysiology were

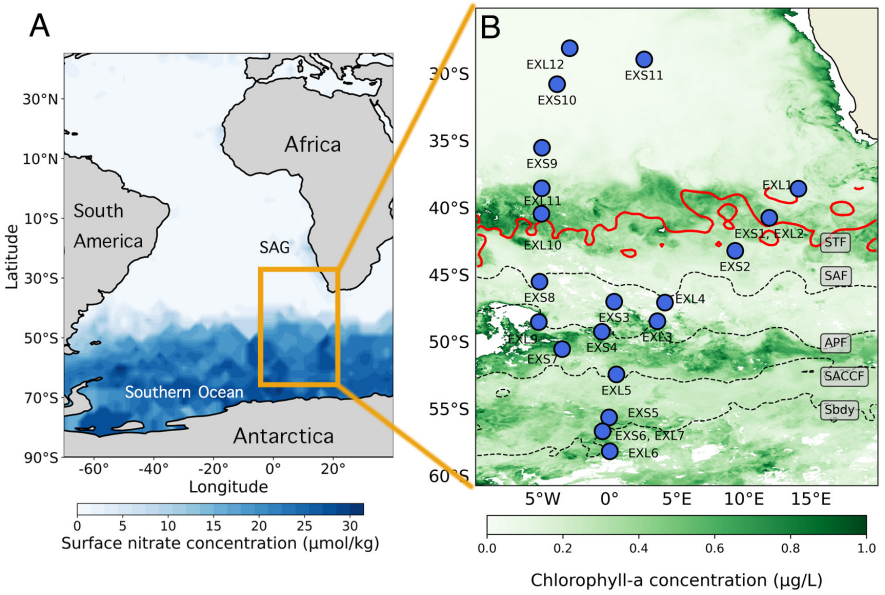

Fig. 1. (*A*) Map showing study area covering the South Atlantic Gyre (SAG) and High Nutrient Low Chlorophyll (HNLC) Southern Ocean with surface nitrate concentration in μmol/kg (World Ocean Atlas Data 2023) (*B*) December 2023–January 2024 Chlorophyll-a concentration in μg/L (Modis AQUA satellite retrievals at 4 km resolution). Fronts from north to south: Sub-Tropical Front- STF (red), Sub-Antarctic Front- SAF, Antarctic Polar Front- APF, Southern Antarctic Circumpolar Current Front- SACCF and Southern boundary- Sbdy. The positions of the fronts were determined by maps of absolute dynamic topography (ADT, m) from the CLS-AVISO product (21) using previously defined boundary definitions (22). Markers indicate the locations where nutrient addition experiments were conducted.

taken at time points of 0, 24, and 48 h after nutrient additions. Photophysiological parameters used in this study are explained in detail (See Materials and Methods and *SI Appendix*, Table S1). From our measurements, dFe concentrations remained below 0.2 nM (*SI Appendix*, Table S2) and limited phytoplankton growth rates south of the STF. Experiments conducted north of the STF were colimited by Fe and N (*SI Appendix*, Fig. S1).

Fe enrichment led to increases in F_v/F_m in all experiments south of the STF (Fig. 2 and *SI Appendix*, Fig. S2). The strongest responses were seen in the APF, where measured dissolved Fe concentrations were less than 0.1 nM (Fig. 2 and *SI Appendix*, Table S1 and Fig. S3). In this region, F_v/F_m increased by 90 to 120% compared to control samples, indicating severe Fe limitation. F_o was reduced by 30 to 45% following Fe addition, while F_m did not change significantly, reflecting decreases in F_m/Chl alongside increasing chlorophyll concentrations. Moreover, the $\sigma_{PSII,}$ reduced by 10 to 20%, within 48 h (*SI Appendix*, Fig. S3).

10 to 25% LHCs Remain Uncoupled from RCs. A linear (R^2= 0.85) inverse relationship between τ and F_v/F_m was observed across all experiments conducted in the study region (Fig. 3*A*), suggesting that as the photosynthetic energy conversion efficiency decreases, more absorbed excitation energy is dissipated via fluorescence (7). Indeed, F_v/F_m was exceptionally low (0.25 ± 0.06) in control treatments, while τ was relatively long (1.37 ± 0.18 ns). After the addition of Fe, F_v/F_m increased to 0.42 ± 0.04 and τ reduced to 0.81 ± 0.09 ns (*SI Appendix*, Table S3). Similar to Fe alone, the supply of Fe in combination with Mn or N also significantly decreased values of τ and increased values of F_v/F_m in all experiments (Fig. 3*A*).

The basic biophysical model for energy distribution in the photosynthetic unit predicts an inverse relationship between the quantum yield of photochemistry (ϕ_P) and the quantum yield of fluorescence (ϕ_F) (8, 20). Using this relationship, the coupling of absorbed excitation energy by LHCs to RCs can be quantified (25, 26). As a result, τ is inversely proportional to the F_v/F_m (*SI Appendix*, Fig. S4). As derived in *SI Appendix*, when all LHCs are coupled,

$$\tau = \tau_m(1 - F_v/F_m), \quad [1]$$

where τ_m averages ca. 1.5 ns in phytoplankton communities of the Southern Ocean (27, 28). If LHC–RCs are energetically coupled, as in nutrient-replete conditions, the results should follow Strasser and Butler's formalism, i.e., Eq. **1** (0% line in Fig. 3*A*). The presence of uncoupled LHCs with extremely long lifetimes increases the fraction of uncoupled LHCs, resulting in a distinct deviation from the classical inverse relationship predicted by Strasser and Butler's model at low F_v/F_m values (Fig. 3*A*). Further modeling this relationship (*SI Appendix*, Fig. S4) to quantify the proportion of uncoupled LHCs revealed that between 10 and 25% of the LHCs are energetically uncoupled from the photochemistry of water splitting in situ (26). The addition of Fe recouples the LHC–RC complexes within 24 h (Fig. 3*B*).

We hypothesized that when Fe was added, LHCs become energetically recoupled to photochemistry before the biochemical repair of inactive RCs. We analyzed the temporal trends in F_v/F_m and τ across three time points (0, 24, and 48 h) (Fig. 3*B*). The experimental results suggest that the uncoupled LHCs decreased to virtually nil in the first phase, within 24 h ($\frac{\Delta\tau_{[0-24h]}}{\Delta(\frac{F_v}{F_m})_{[0-24h]}} = -5.55$).

Moreover, after 24 h, the experimental results are consistent with Strasser and Butler's model of photosynthetic energy efficiency; approximately 54% of the absorbed excitation energy is thermally dissipated (7, 8). The reduced slope during the latter phase

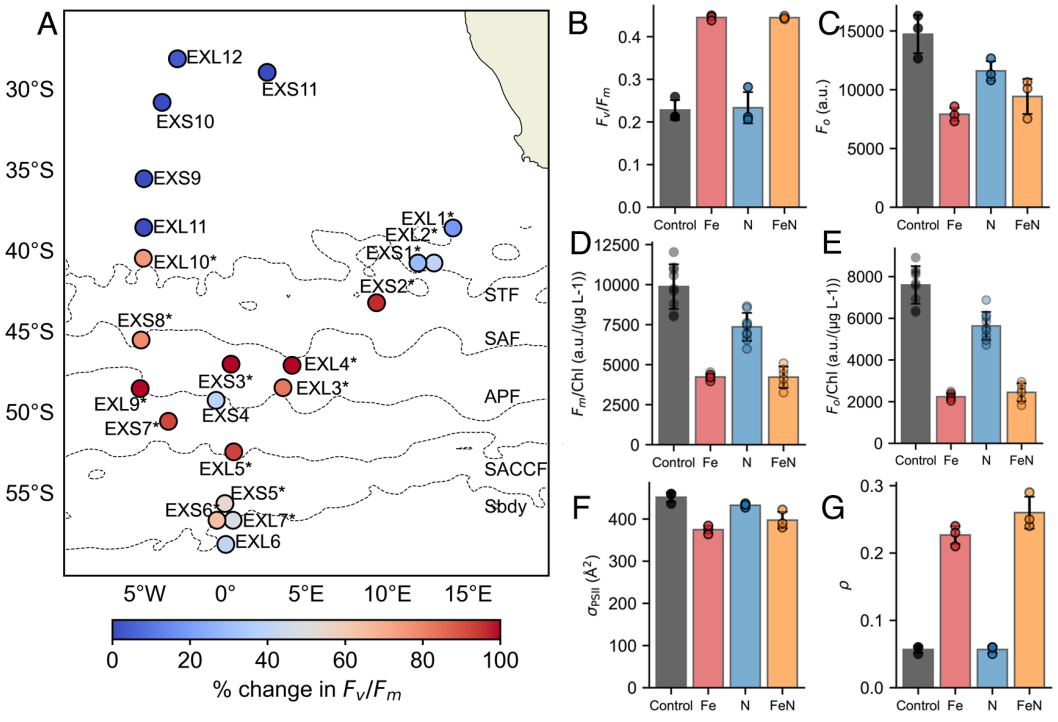

Fig. 2. (*A*) Spatial distribution of percentage change in F_v/F_m in incubation experiments 48 h after Fe addition to final concentrations of 2 nM. Experiments where statistically significant results were obtained are indicated by * based on results of ANOVA followed by Tukey Honest Significant Difference post hoc test. ($P \leq 0.05$). Markers used for experiments indicate the percentage size of response observed in F_v/F_m upon Fe addition according to provided color scale. The approximate latitudes of the STF, SAF, APF, SACCF, and the Sbdy are indicated by dotted lines. Example responses of photo physiological parameters, (*B*) F_v/F_m, (*C*) F_o (*D*) Maximal fluorescence per chlorophyll concentration F_m/Chl, (*E*) Minimal fluorescence per chlorophyll concentration F_o/Chl, (*F*) σ_{PSII}, and (*G*) ρ, 48 h after nutrient amendments of Control (black), Fe only (red), N only (blue) and Fe, N (orange) in experiment EXS7.

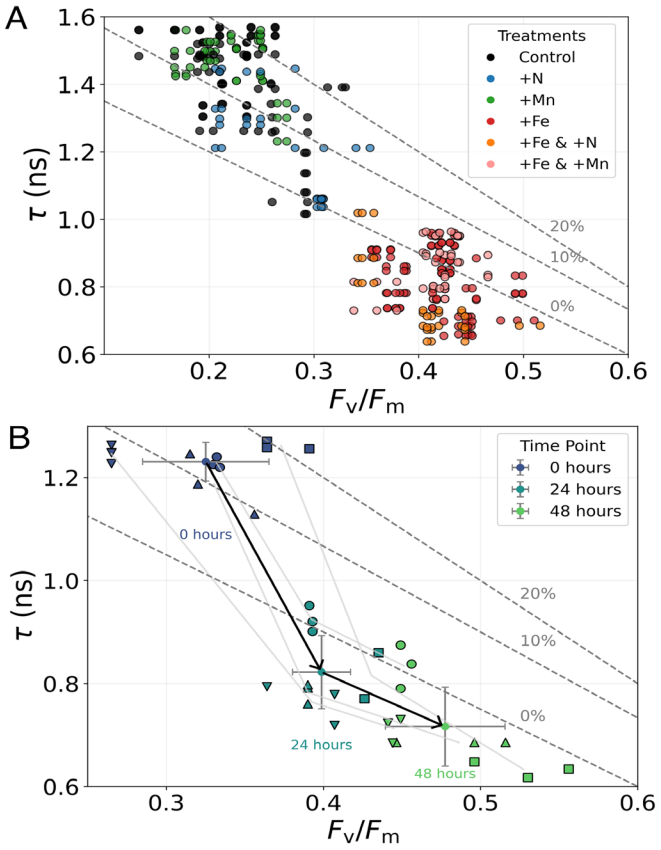

Fig. 3. (*A*) Relationship between fluorescence lifetimes and F_v/F_m after 48 h of nutrient additions in Fe-stressed regions. The gray line with 0% mark is the theoretical dependence between the fluorescence lifetime and F_v/F_m. Gray lines (labeled as 10 to 20%) are the modeled dependence between F_v/F_m and τ, when 10 to 20% of the LHCs are energetically decoupled from the photosynthetic RCs (Derivation included in *SI Appendix*). (*B*) Temporal trends in the changes of F_v/F_m and τ in response to Fe addition in experiments EXS3 (circle marker), EXS5 (square marker), EXS6 (triangle marker), EXS7 (inverted triangle marker).

between 24 to 48 h, ($\frac{\Delta\tau_{[24-48h]}}{\Delta(\frac{F_v}{F_m})_{[24-48h]}} = -1.35$) indicates a deceleration in these changes, potentially due to the stabilization of LHC–RC complexes and the biophysical recovery of inactive RCs.

Discussion

The results of our analysis reveal that a large fraction of LHCs is energetically uncoupled from photochemistry in situ in the South Atlantic Ocean due to Fe-stress. Variable fluorescence measurements have been used in previous field studies conducted in the High Nutrient Low Chlorophyll (HNLC) waters to conclude that Fe stress leads to a significant reduction in photosynthetic efficiency (29, 30). However, these measurements alone cannot accurately quantify the presence of uncoupled antenna complexes. The current study uses the combination of fluorescence efficiency and lifetimes within Fe addition experiments to directly assess the effects of Fe stress on energy coupling in natural marine phytoplankton assemblages in situ.

The changes we observed in F_v/F_m, F_o, F_m, σ_{PSII}, and ρ suggest (1) that a significant portion of LHCs are energetically uncoupled from RCs in Fe-limited waters of the study region, and (2) these complexes can rapidly recouple upon the addition of Fe. Our results clearly reveal that F_v/F_m increases following Fe addition, due to a decrease in F_o. Similar observations in laboratory cultures of a unicellular red alga, *Rhodella violacea*, led Desquilbet et al. to conclude that an increase in F_o under Fe stress cannot be attributed solely to an increase in PSII, as this would also lead to a comparable rise in F_v (17). Instead, these authors suggested that a disproportionately large increase in F_o compared to F_v results in a greater contribution from the Photosystem I (PSI)-LHC complex to the F_o signal. However, natural marine phytoplankton assemblages contain extremely low concentrations of red algae, and fluorescence from PSI at physiological temperatures is negligible, with virtually all fluorescence associated with PSII. Previous studies on cyanobacteria have associated the observed rise in F_o and increased τ to the accumulation of stress-induced chlorophyll-binding proteins (e.g., IsiA) or from degradation of PSII RCs, leaving excess LHCs unable to transfer energy (16, 31). HNLC regions of the ocean are dominated by diatom populations, and Fe resupply has shown a significant increase in diatom abundance and biomass in Fe fertilization experiments conducted in these regions (32). The isiA gene, primarily found in cyanobacteria (33), has not been found in the diatom genome (34). Concerning diatoms, iron starvation-induced proteins have been detected; however, the localization of these protein structures is not fully understood (35). Moreover, although the presence of inactive RCs can be responsible for longer τ, the shift from the Strasser and Butler's 0% reference line (Fig. 3*A*) much longer τ's coupled with lower F_v/F_m cannot be explained only by the presence of inactive RCs (20).

We thus proffer an alternative explanation: We propose that the changes observed on F_o(/Chl) and F_m(/Chl) upon Fe addition in situ represent recoupling of LHCs to PSII RCs. In theory, F_m is the fluorescence when the acceptor side of PSII RCs is reduced (i.e., "closed"). Under this condition, photochemistry is nil, and absorbed photons are dissipated as heat or fluorescence. When LHCs are energetically recoupled to RCIIs through the addition of Fe, F_m did not change significantly and F_o(/Chl) decreased. Moreover, Fe limitation increases the fraction of inactive RCs, thus increasing the physical distance between the remaining active RCs and reducing the probability of exciton transfer between them, as evidenced by extremely low values of ρ (Fig. 2*G*). Fe enrichment leads to the repair of inactive centers and the recovery in ρ (Figs. 2*G* and 4*D*).

Fe stress also significantly influences the PSII functional absorption cross section, σ_{PSII} (Figs. 2*F* and 4*C*). Upon addition of Fe, a pronounced increase in σ_{PSII} was observed at 24 h in EXS2 and EXS8, in the Sub-Antarctic zone, suggesting an initial response to Fe supplementation (Fig. 4*C* and *SI Appendix*, Fig. S5). Notably, EXS2 and EXS8 exhibited the lowest F_v/F_m (0.230 ± 0.004, 0.231 ± 0.009) values and the longest τ (1.269 ± 0.144 ns, 1.175 ± 0.060 ns) values, respectively, indicating that these locations experienced the most severe Fe stress in the studied area. Vassilev et al. reported changes to σ_{PSII} upon addition of Fe to Fe-stressed cultures of the green alga, *Dunaliella tertiolecta* (18). Similar to our observations, they observed that, under extreme limitation, σ_{PSII} and F_v/F_m were initially low, but increased rapidly to their respective maxima, upon addition of Fe; σ_{PSII} subsequently declined while F_v/F_m remained elevated. Both σ_{PSII} and F_v/F_m then reached steady-state levels after ca. 30 h at room temperature (18). Both these results and the findings presented here (Fig. 4 *A–D*) thus indicate that, under Fe limitation, LHCs are coupled to the few remaining functional PSII RCs, reducing the probability of exciton energy transfer from LHCs to the RCs, due to the weakened interaction with its acceptor-side chlorophyll molecules of the RC; this is a so-called "puddle" model of excitation transfer (Fig. 4*E*) (36). This may cause inefficient excitation energy transfer in the uncoupled LHCs, where energy will be lost before reaching the RC, reducing the measured σ_{PSII}, and increasing τ, under Fe stress (Fig. 4 *B* and *C*).

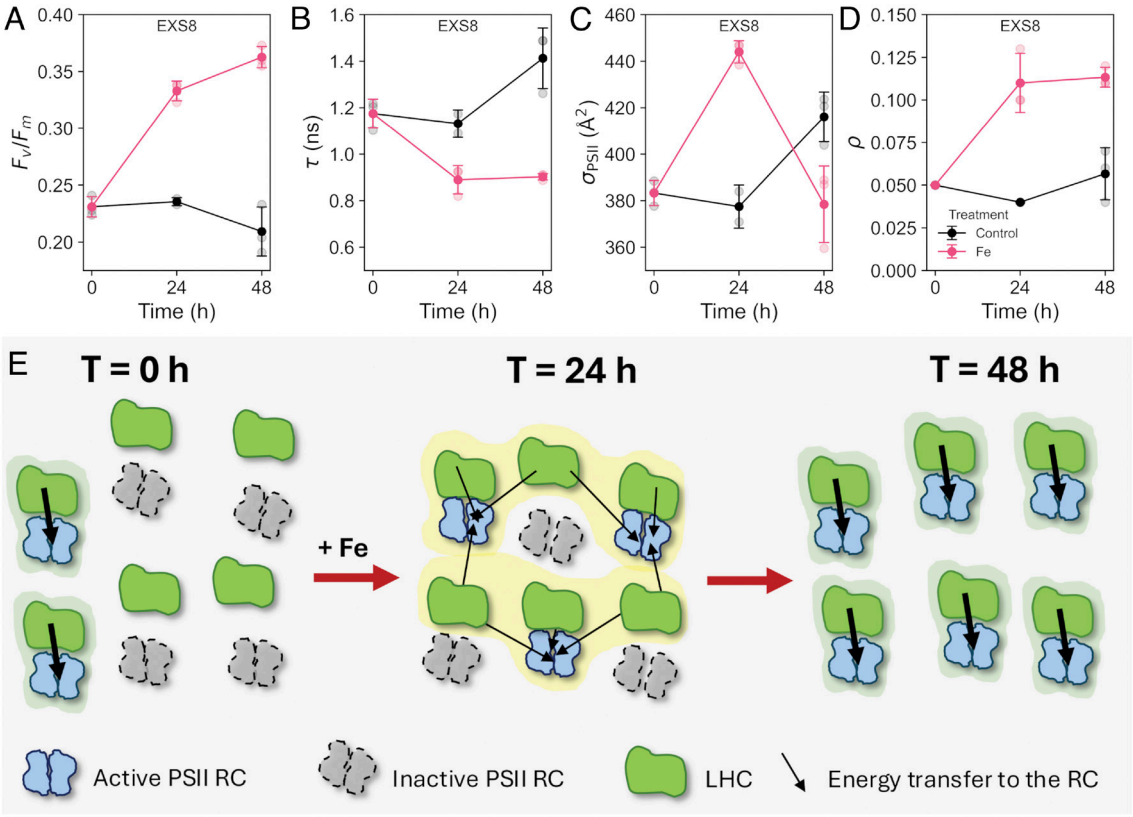

Fig. 4. Example responses in (*A*) F_v/F_m, (*B*) τ, (*C*) σ_{PSII}, and (*D*) ρ, with time (T = 0 h, T = 24 h, and T = 48 h) following the addition of Fe in experiment EXS8 (see *SI Appendix*, Fig. S5 for comparable plot from EXS2) (*E*) Schematic representation of modifications in the photosynthetic machinery upon transition from Fe-stressed to nutrient-replete conditions.

The initial increase of σ_{PSII} over the first 24 h (Fig. 4*C*) can be then explained by the rapid reconnection of uncoupled LHCs to photochemically functional domains, causing an apparent enhancement of the size of the photosynthetic unit, explained as the "lake" model (Fig. 4 *C* and *E*). This change is then followed by the addition of newly activated or synthesized RCs, which reduces the effective cross section of the antenna serving RCs. Indeed, a significant decline in σ_{PSII} (T = 24 to T = 48 h) was detected, mirroring the latter phase (Fig. 4*C*) as previously observed in the culture (18). Notably, experiments conducted in the Sub-Antarctic zone (Figs. 2 and 4), appeared to be the most severely Fe-stressed in these conditions; the rest exhibit a more moderate Fe stress response. Experiments conducted in the South Atlantic gyre, north of the Sub-Tropic Front indicated N limitation (*SI Appendix*, Fig. S1), suggesting that N stress affects photosynthesis differently. In contrast to the Fe addition response observed in Fe-stressed waters, addition of N to N-stressed waters increased σ_{PSII} and F_m, due to increased chlorophyll (i.e. LHC) synthesis.

Combining the $ø_P$ from variable fluorescence and $ø_F$ from picosecond lifetime measurements, we quantified the fraction of uncoupled LHCs, estimating that between 10 and 25% of the antenna complexes are energetically uncoupled. Diel studies conducted by Park et al. (26) in the Amundsen Sea polynyas (Antarctica) recorded fluorescence lifetimes in the range of 0.7 to 1.3 ns in the absence of Fe stress with up to 25% LHCs uncoupled. Sherman et al. (37) examined diel changes in photosynthetic parameters in the Equatorial Atlantic, where they showed that 25 to 40% of LHC–RC complexes remain uncoupled and that they recouple due to upwelling. However, these efforts lacked direct Fe manipulations, trace metal clean methodology, and measurements of Fe concentrations, therefore, it was not possible to fully link observed photophysiological changes to Fe limitation.

The combined results of the fluorescence lifetimes and observations of σ_{PSII}, included within direct experimental manipulations, indicate that the region of study was subjected to Fe stress, and we were able to validate that changes observed in variable fluorescence were indeed due to LHC–RC uncoupling and not confounded by alternative photophysiological processes. Prior studies (e.g., ref. 29) that estimated proportions of uncoupled LHCs have largely used models derived from only variable fluorescence. While responses in variable fluorescence parameters are more commonly used to deduce reasons behind photophysiological changes, they provide only indirect evidence of excitation energy transfer. In contrast, fluorescence lifetime measurements provide a direct way to measure the $ø_F$ and assess the energy dissipation state of the photosynthetic machinery more accurately. Therefore, this approach provides an accurate mechanistic understanding of Fe stress responses in natural phytoplankton communities and represents an important methodological advancement for in situ oceanographic studies.

Our results provide a demonstration of in situ temporal dynamics of the interactions between LHC–RC complexes and the restoration of photosynthetic function upon Fe resupply. Further, t experimental data strongly suggest that restabilization of photosynthesis upon Fe addition is multifaceted. First, the recoupling of LHC–RC complexes results in a significantly higher rate of change of τ than F_v/F_m, as a response to Fe addition to Fe-stressed phytoplankton. Within the first 24 h of Fe addition, data points migrate to the Strasser and Butler's 0% reference line, while reducing the percentage of uncoupled LHCs, with higher changes in fluorescence lifetime than $F_v/F_{m,}$ (Fig. 3*B*) suggesting that spatial changes in distance or orientation of RC and LHCs is responsible for the recoupling and reduction of fluorescence emission during this phase. Nunn et al. (38) conducted quantitative proteomics

in a diatom under Fe stress, indicating the loss of RCs. Moreover, studies have shown that Fe limitation led to a loss of PSII subunits D1, CP43, and CP47 and a gain of D2 and $cytb_{559}$, in isolated thylakoid membranes (15, 18, 29, 38). Repair of these components upon Fe addition implies the recoupling and stabilization of LHC–RC complexes and stabilization of LHC–RC complexes as shown by the higher rate of change of F_v/F_m during the second phase between 24 to 48 h, where data points follow the Strasser and Butler's relationship.

Why Do Phytoplankton Have a Pool of Uncoupled LHCs? The value to phytoplankton of producing a large pool of uncoupled antenna under Fe-stress is not well understood. Due to the large size of photosynthetic machinery and the complexity of intermolecular interactions between its subunits, a growing number of in vitro and in silico experiments have been conducted to study intramolecular energy transfer in isolated photosynthetic proteins, especially LHCs (39, 40). Laboratory-based studies imply that LHC–RC supercomplexes are highly variable; subjecting these cells to various changes can result in PSII cores with different amounts of LHCs and minor light-harvesting proteins attached. The heterogeneity of PSII RCs in nutrient-replete conditions within thylakoid membranes has been visualized by using phase contrast cryoelectron tomography by Levitan et al (41). They provided proof of two distinct subpopulations of PSII RCs associated with and without LHCs in thylakoid membranes isolated from *Phaeodactylum tricornutum* and proposed that RCs unassociated with LHCs serve as physically isolated repair stations where photochemically damaged proteins (e.g., D1) can be removed and replaced with functional structures (41).

Uncoupled RCs may help protect the photosynthetic apparatus from photodamage. If LHC–RCs remain coupled, excess light energy can accumulate in the photosystem without being utilized effectively and may thus increase the risk of photodamage. To reduce such damage, phytoplankton may uncouple their LHCs from RCs to reduce energy capture, resulting in less energy needs to be processed downstream in the electron transport chain. Under Fe-stress, phytoplankton need to optimize the balance between energy absorption and the capability of the photosynthetic machinery to use that energy effectively. Subsequent steps in the photosynthetic electron transport chain also have high requirements for Fe. The reduced energetic connectivity between LHC–RCs can help to prevent energy imbalance by maintaining the rate of excitation at the PSII RC chlorophylls, more in line with the reduced rate of electron transfer, which is hindered by limited Fe. Sudden environmental changes such as light intensity or nutrient fluxes can occur on faster timescales than protein and pigment turnover rates. Therefore, uncoupled LHCs may also serve as a pigment reserve which can rapidly increase photosynthetic efficiency under conditions of Fe supply (16, 42).

Our results suggest that the uncoupled antenna produced under Fe limitation can significantly influence the energy balance of phytoplankton in the ocean and thereby affect the overall primary production of the South Atlantic Ocean, emphasizing the need for the incorporation of in situ and in vivo fluorescence studies to accurately understand how nutrient availability affects photosynthetic machinery in marine phytoplankton and the importance of understanding the reasons and mechanisms behind the uncoupling phenomenon.

Materials and Methods

Nutrient Additions Experiments. The cruise track facilitated nutrient addition experiments to be conducted over a large temperature gradient and range of both dissolved macronutrient and dFe concentrations (*SI Appendix*, Table S1). Nutrient addition experiments were set up and conducted under trace metal clean conditions in a class-100 clean air laboratory container as explained in detail by Wyatt et al. (43). Surface seawater (2 to 3 m) for experiments was pumped directly into the clean laboratory using a Teflon diaphragm pump (A-15, Almatec) connected by acid-washed PVC tubing to a towed "Fish" sampler. Samples for initial (T_0) measurements (photophysiology, chlorophyll a, and macronutrients) were collected at the beginning, middle (i.e., after all experimental bottles were ~50% full), and end of the filling process, with dFe (0.2 μm) samples also collected at the beginning and end. Separate replicate bottles were amended with single or combination additions of Fe and Mn, to final concentrations of 2 nM using $FeCl_3$ and $MnCl_2$, respectively, and prepared following the detailed procedure in ref. 43. N and P were added as 10 mM KNO_3/10 mM NH_4Cl and 1 mM $NaHPO_4$ to a final concentration of 1 μM. Combinations of Fe, Mn were used in experiments conducted in the South Antarctic Zone, and further south, and Fe, N when in the SAG. Control bottles, with no added nutrients, were collected in parallel. Following nutrient amendment, the bottles were closed, then externally sealed with film (Parafilm™) and incubated in a temperature-controlled container set to approximate sea surface temperature of the stations ranging from 6.0 to 24.0 °C (*SI Appendix*, Table S2). The incubation environment was maintained using daylight simulation LED light banks with ~200 μmol photons m^{-2} s^{-1} flux and set to an approximate local day/night cycle of 16 and 8 h, respectively.

Dissolved Iron Measurements. Flow injection analysis with chemiluminescence detection (FIA-CL) was used to determine nanomolar concentrations of dFe in the nutrient addition experiments (44). Briefly, each sample was spiked 1 h prior to analysis with 60 μL 0.01 M H_2O_2 and left to equilibrate, to allow any present Fe(II) to be oxidized to Fe(III) (45). The sample was then buffered in-line to pH 3.5, and preconcentrated onto the cation exchange resin Toyopearl-AF-Chelate 650 M (Tosohaas). Following a rinse step of 0.013 M HCl to remove the bulk seawater matrix, the Fe(III) was liberated from the resin using 0.24 M HCl and entered the reaction stream with luminol, NH_4OH and H_2O_2 to induce the chemiluminescent oxidation of luminol, detected by a photomultiplier tube. Each sample was measured in triplicate, with a detection limit (3σ) of 0.05 ± 0.02 nM (n = 11). Accuracy was established by repeat quantification of dFe in an internal reference standard (ZIPLOC 1; 0.3 nM), yielding a concentration of 0.34 ± 0.02 nM (n = 7), which agrees with the consensus value.

Variable Fluorescence and Picosecond Lifetime Fluorescence. Photophysiology measurements were conducted at time points of T = 24, T = 32, T = 48 h in short experiments ("EXS") and T = 48, T = 96 h in large experiments ("EXL") to assess short-term and long-term responses. Measurements included 3 technical replicates for each biological replicate (i.e., each bottle). Variable chlorophyll fluorescence measurements were made using a Fluorescence Induction Relaxation (FIRe) instrument (46). A saturating single turnover flash (STF) from blue light-emitting diodes (450 ± 30 nm half bandwidth) was used to cumulatively reduce all PSII RCs within ca. 80 μs. Data from the FIRe were analyzed to derive values of the minimum and maximum fluorescence (F_o and F_m, respectively) and the photochemical efficiency of photosystem II, $ø_P$,

$$ø_P = F_v / F_m, \text{ where } F_v = (F_m - F_o).$$

Functional absorption cross section of PSII (Å^2) in a dark-adapted state, σ_{PSII} (at 450 nm), was calculated by fitting the fluorescence rise to a cumulative one-hit Poisson function. σ_{PSII} is the product of the optical absorption cross section of PSII (i.e., the physical size of the PSII unit) and the quantum yield of photochemistry in PSII. "Connectivity factor", ρ is a parameter that defines the excitation energy transfer between individual photosynthetic units of PSII (dimensionless).

The PicoLiF fluorometer was used to record fluorescence kinetics in open photosynthetic RCs. The kinetic signal at the F_o level (τ) was induced by laser excitation with low average optical power density of 0.1 mW·cm^{-2} (23). The PicoLiF measured picosecond fluorescence decays which were deconvoluted from the instrument response function and then fitted to a sum of three exponentials with a custom TCSPFIT Matlab package (47). The quantum yield of fluorescence $ø_F$ was then calculated from,

$$ø_F = \tau_{observed} / \tau_{natural},$$

$\tau_{observed}$ is the measured lifetime and $\tau_{natural}$ is the natural lifetime of a chlorophyll a molecule (48, 49). $\tau_{natural}$ is the time that would be required for a molecule to

return to the ground state from an excited state if fluorescence were the sole dissipation pathway. For Chl a, $\tau_{natural}$ is 15 ns and is constant, independent of solvent, organism, or environmental condition (25). Percentage change was calculated as $\frac{(\text{Fe Treatment}_{48h} - \text{Control}_{48h})}{\text{Control}_{48h}} \times 100\%$ (Fig. 2*A* and *SI Appendix* Fig. S3). Differences between the various response variables within the experiments were assessed using ANOVA followed by a Tukey's HSD comparison test ($P < 0.05$)

Data, Materials, and Software Availability. All study data are included in the article and/or *SI Appendix*.

ACKNOWLEDGMENTS. We thank the captain, officers, and crew of the RRS *Discovery* cruise DY172. This work was funded by the Bennett L. Smith Endowment awarded to P.G.F. and the Natural Environment Research Council UK Project "A New Perspective on Ocean Photosynthesis"(N-POP) (Grant NE/W000903/1) awarded to T.S.B., C.M.M., and M.C.L.T.J.R.-K. was supported through the Council for Scientific and Industrial Research's (CSIR) Southern Ocean Carbon-Climate Observatory funded by the Department of Science and Innovation (DSI/CON C3184/2023), the CSIR's Parliamentary Grant (0000005278), and the National Research Foundation South African National Antarctic Programme (SANAP23042496681).

Author affiliations: [a]Department of Chemistry and Chemical Biology, Rutgers University, New Brunswick, NJ 08854; [b]Environmental Biophysics and Molecular Ecology Program, Department of Marine and Coastal Sciences, Rutgers University, New Brunswick, NJ 08901; [c]School of Ocean and Earth Science, National Oceanography Centre, Southampton, University of Southampton, Southampton SO14 3ZH, United Kingdom; and [d]Southern Ocean Carbon-Climate Observatory, Council for Scientific and Industrial Research, Cape Town 7700, South Africa

1. P. G. Falkowski, *Aquatic Photosynthesis* (Princeton University Press, ed. 2, 2007).
2. R. E. Blankenship, *Molecular Mechanisms of Photosynthesis* (Blackwell Science, ed. 1, 2002).
3. R. Croce, H. van Amerongen, Natural strategies for photosynthetic light harvesting. *Nat. Chem. Biol.* **10**, 492–501 (2014).
4. T. Forster, Energiewanderung und Fluoreszenz. *Naturwissenschaften* **33**, 166–175 (1946).
5. T. Mirkovic *et al.*, Light Absorption and energy transfer in the antenna complexes of photosynthetic organisms. *Chem. Rev.* **117**, 249–293 (2017).
6. E. Belgio, M. P. Johnson, S. Juric, A. V. Ruban, Higher plant photosystem II light-harvesting antenna, not the reaction center, determines the excited-state lifetime-both the maximum and the nonphotochemically quenched. *Biophys. J.* **102**, 2761–2771 (2012).
7. W. L. Butler, R. J. Strasser, Tripartite model for the photochemical apparatus of green plant photosynthesis. *Proc. Natl. Acad. Sci. U.S.A.* **74**, 3382–3385 (1977).
8. W. L. Butler, Energy distribution in the photochemical apparatus of photosynthesis. *Ann. Rev. Plant Physiol.* **29**, 345–378 (1978).
9. S. Izawa, N. E. Good, Effect of salts and electron transport on the conformation of isolated chloroplasts. II. Electron microscopy. *Plant Physiol.* **41**, 544–552 (1966).
10. A. V. Ruban, M. P. Johnson, Visualizing the dynamic structure of the plant photosynthetic membrane. *Nat. Plants* **1**, 15161 (2015).
11. L. M. Wlodarczyk *et al.*, Functional rearrangement of the light-harvesting antenna upon state transitions in a green alga. *Biophys. J.* **108**, 261–271 (2015).
12. M. Y. Gorbunov, P. G. Falkowski, Using chlorophyll fluorescence to determine the fate of photons absorbed by phytoplankton in the world's oceans. *Annu. Rev. Mar. Sci.* **14**, 213–238 (2022).
13. M. J. Behrenfeld, A. J. Milligan, Photophysiological expressions of iron stress in phytoplankton. *Annu. Rev. Mar. Sci.* **5**, 217–246 (2013).
14. H. C. Riethman, L. A. Sherman, Purification and characterization of an iron stress-induced chlorophyll-protein from the cyanobacterium. *Anacystis nidulans* R2. *Biochim. Biophys. Acta* **935**, 141–151 (1988).
15. R. M. Greene, R. J. Geider, P. G. Falkowski, Effect of iron limitation on photosynthesis in a marine diatom. *Limnol. Oceanogr.* **36**, 1772–1782 (1991).
16. T. J. Ryan-Keogh, A. I. Macey, A. M. Cockshutt, C. M. Moore, T. S. Bibby, The cyanobacterial chlorophyll-binding-protein IsiA acts to increase the in vivo effective absorption cross-section of PSII under iron limitation. *J. Phycol.* **48**, 145–154 (2012).
17. T. E. Desquilbet, D. Jean-Claude, B. Robert, J. Houmard, J. C. Thomas, In the unicellular red alga *Rhodella violacea* iron deficiency induces an accumulation of uncoupled LHC. *Plant Cell Physiol.* **44**, 1141–1151 (2003).
18. I. R. Vassiliev *et al.*, Effects of iron limitation on photosystem II composition and light utilization in *Dunaliella teutiolecta*. *Plant Physiol.* **109**, 963–972 (1995).
19. J. L. Moseley *et al.*, Adaptation to Fe-deficiency requires remodeling of the photosynthetic apparatus. *EMBO J.* **21**, 6709–6720 (2002).
20. H. Lin *et al.*, The fate of photons absorbed by phytoplankton in the global ocean. *Science* **351**, 264–267 (2016).
21. M. H. Rio, S. Guinehut, G. Larnicol, New CNES-CLS09 global mean dynamic topography computed from the combination of GRACE data, altimetry, and in situ measurements. *J. Geophys. Res. Oceans* **116**, 1–25 (2011).
22. S. Swart, S. Speich, I. J. Ansorge, J. R. E. Lutjeharms, An altimetry-based gravest empirical mode south of Africa: 1. Development and validation. *J. Geophys. Res. Oceans.* **115**, 1–19 (2010).
23. M. Y. Gorbunov, P. G. Falkowski, Using picosecond fluorescence lifetime analysis to determine photosynthesis in the world's oceans. *Photosynth. Res.* **159**, 253–259 (2024).
24. M. J. Behrenfeld *et al.*, Satellite-detected fluorescence reveals global physiology of ocean phytoplankton. *Biogeosciences* **6**, 779–794 (2009).
25. M. A. Palacios, F. L. de Weerd, J. A. Ihalainen, R. van Grondelle, H. van Amerongen, Superradiance and exciton (de)localization in light-harvesting complex II from green plants. *J. Phys. Chem. B* **106**, 5782–5787 (2002).
26. J. Park *et al.*, Light availability rather than Fe controls the magnitude of massive phytoplankton bloom in the Amundsen Sea polynyas Antarctica. *Limnol. Oceanogr.* **62**, 2260–2276 (2017).
27. F. I. Kuzminov, M. Y. Gorbunov, Energy dissipation pathways in photosystem 2 of the diatom, *Phaeodactylum tricornutum*, under high-light conditions. *Photosynth. Res.* **127**, 219–235 (2016).
28. J. Sherman, M. Y. Gorbunov, O. Schofield, P. G. Falkowski, Photosynthetic energy conversion efficiency in the West Antarctic Peninsula. *Limnol. Oceanogr.* **65**, 2912–2925 (2020).
29. P. G. Falkowski, R. M. Greene, R. J. Geider, Physiological limitations on phytoplankton productivity in the ocean. *Oceanography* **5**, 84–91 (1992).
30. R. M. Greene, Z. S. Kolber, D. G. Swift, N. W. Tindale, P. G. Falkowski, Physiological limitation of phytoplankton photosynthesis in the eastern equatorial Pacific determined from variability in the quantum yield of fluorescence. *Limnol. Oceanogr.* **39**, 1061–1074 (1994).
31. R. L. Burnap, T. Troyan, L. A. Sherman, The highly abundant chlorophyll-protein complex of iron-deficient *Synechococcus* sp. PCC7942 (CP43') is encoded by the isiA gene'. *Plant Physiol.* **103**, 893–902 (1993).
32. H. J. W. Baar *et al.*, Synthesis of iron fertilization experiments: From the iron age in the age of enlightenment. *J. Geophys. Res. Oceans* **110**, 2004JC002601 (2005).
33. U. Geiss *et al.*, Detection of the isiA gene across cyanobacterial strains: potential for probing iron deficiency. *Appl. Environ. Microbiol.* **67**, 5247–5253 (2001).
34. C. Bowler *et al.*, The *Phaeodactylum* genome reveals the evolutionary history of diatom genomes. *Nature* **456**, 239–244 (2008).
35. E. Kazamia *et al.*, In vivo localization of iron starvation induced proteins under variable iron supplementation regimes in *Phaeodactylum tricornutum*. *Plant Direct* **6**, e472 (2022).
36. K. Bernhardt, H. W. Trissl, Theories for kinetics and yields of fluorescence and photochemistry: How, if at all, can different models of antenna organization be distinguished experimentally?. *Biochim. Biophys. Acta* **1409**, 125–142 (1999).
37. J. Sherman *et al.*, The photophysiological response of nitrogen-limited phytoplankton to episodic nitrogen supply associated with tropical instability waves in the Equatorial Atlantic. *Front. Mar. Sci.* **8**, 1–14 (2022).
38. B. L. Nunn *et al.*, Diatom proteomics reveals unique acclimation strategies to mitigate Fe limitation. *PLoS ONE* **8**, e75653 (2013).
39. E. Kim, S. Akimoto, R. Tokutsu, M. Yokono, J. Minagawa, Fluorescence lifetime analyses reveal how the high light-responsive protein LHCSR3 transforms PSII light-harvesting complexes into an energy-dissipative state. *J. Biol. Chem.* **292**, 18951–18960 (2017).
40. S. Caffarri, K. Broess, R. Croce, H. van Amerongen, Excitation energy transfer and trapping in higher plant Photosystem II complexes with different antenna sizes. *Biophys. J.* **100**, 2094–2103 (2011).
41. O. Levitan *et al.*, Structural and functional analyses of photosystem II in the marine diatom Phaeodactylum tricornutum. *Proc. Natl. Acad. Sci. U.S.A.* **116**, 17316–17322 (2019).
42. M. J. Behrenfeld *et al.*, Controls on tropical Pacific Ocean productivity revealed through nutrient stress diagnostics. *Nature* **442**, 1025–1028 (2006).
43. N. J. Wyatt *et al.*, Phytoplankton responses to dust addition in the Fe-Mn co-limited eastern Pacific sub-Antarctic differ by source region. *Proc. Natl. Acad. Sci. U. S. A.* **120**, e2220111120 (2023).
44. K. Kunde *et al.*, Iron distribution in the Subtropical North Atlantic: The pivotal role of colloidal iron. *GBC* **33**, 1532–1547 (2019).
45. M. C. Lohan, A. M. Aguilar-Islas, K. W. Bruland, Direct determination of iron in acidified (pH 1.7) seawater samples by flow injection analysis with catalytic spectrophotometric detection: Application and intercomparison. *Limnol. Oceanogr. Methods* **4**, 164–171 (2006).
46. M. Y. Gorbunov, P. G. Falkowski, Using chlorophyll fluorescence kinetics to determine photosynthesis in aquatic ecosystems. *Limnol. Oceanogr.* **66**, 1–13 (2021).
47. J. Enderlein, R. Erdmann, Fast fitting of multi-exponential decay curves. *Opt. Commun.* **134**, 371–378 (1997).
48. J. R. Lakowicz, *Principles of Fluorescence Spectroscopy* (Springer, ed. 3, 2010).
49. S. S. Brody, E. Rabinowitch, Excitation lifetime of photosynthetic pigments in vitro and in vivo. *Science* **125**, 555 (1957).